

- [7] a) P. B. O'Donnell, J. W. McGinity, *Adv. Drug Delivery Rev.* **1997**, *28*, 25–42.  
 [8] R. P. Haugland, *Handbook of Fluorescent Probes and Research Chemicals*, 6th ed., Molecular Probes, Eugene, OR, **1996**, p. 29.  
 [9] As determined by differential scanning calorimetry (DSC).  
 [10] B. A. Demeneix, J.-P. Behr in *Artificial Self-Assembling Systems for Gene Delivery* (Eds.: P. L. Felgner, M. J. Heller, P. Lehn, J. P. Behr, F. C. Szoka, Jr.), American Chemical Society, Washington, DC, **1996**, pp. 146–151.  
 [11] a) M. Singh, M. Briones, G. Ott, D. O'Hagan, *Proc. Natl. Acad. Sci. USA* **2000**, *97*, 811–816; b) S. Ando, D. Putnam, D. W. Pack, R. Langer, *J. Pharm. Sci.* **1999**, *88*, 126–130; c) M. L. Hedley, J. Curley, R. Urban, *Nat. Med.* **1998**, *4*, 365–368.

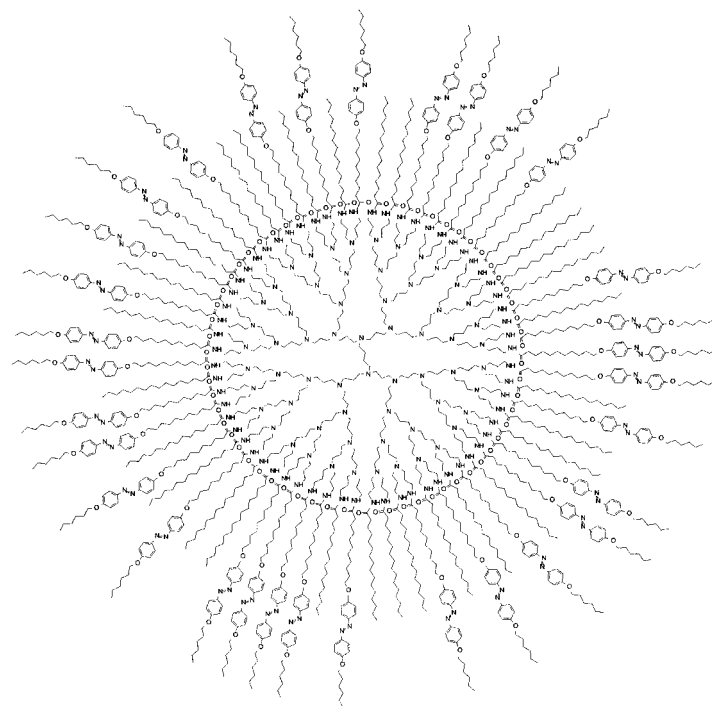
## Merging of Hard Spheres by Phototriggered Micromanipulation\*\*

Georg C. Dol, Kenji Tsuda, Jan-Willem Weener, Marcel J. Bartels, Theodor Asavei, Thomas Gensch, Johan Hofkens, Loredana Latterini, Albert P. H. J. Schenning, Bert W. Meijer, and Frans C. De Schryver\*

Amphiphilic dendrimers, namely those that carry both hydrophobic and hydrophilic regions within one molecule, tend to self-assemble into a large variety of different aggregates depending on their structure. The dendritic amphiphiles investigated so far include unimolecular micelles,<sup>[1]</sup> bolaamphiphiles,<sup>[2]</sup> dendronized polymers,<sup>[3]</sup> super-amphiphiles,<sup>[4]</sup> and various other AB and ABA block copolymers.<sup>[5]</sup> Poly(propyleneimine) dendrimers modified with aliphatic end groups proved to be extremely flexible. Protonation of the amine core (for example, by water) resulted in these dendrimers acting as amphiphiles in which all (64 for the fifth generation) the aliphatic tails point to one side while the dendrimer core adjusts its conformation to form a nearly flat structure.<sup>[1f]</sup> Recently, the use of photoresponsive (dendritic) building blocks, obtained through the incorporation of azobenzene units, led to the formation of photo-switchable monolayers, whose macroscopic properties could be completely controlled by irradiation.<sup>[6]</sup> Here we describe

how the use of amphiphilic azobenzene-modified dendrimers can give rise to the formation of photoresponsive supramolecular assemblies. With the aid of micromanipulation techniques, these well-defined supramolecular aggregates of dendrimers were subsequently used as secondary building blocks in the formation of even larger objects, with dimensions in the micrometer regime. Consequently, the structures ultimately obtained are the result of tuning at three different length scales.

We will focus on the fifth generation azobenzene-containing alkyl-modified poly(propyleneimine) dendrimer **1** (Scheme 1), an amphiphilic blockcopolymer with a random



Scheme 1. Schematic representation of azobenzene-modified dendrimer **1**, to illustrate the random character of the attachment of the azobenzene and palmitoyl units at the rim of the dendrimer.

shell structure that carries on average 32 azobenzene groups and 32 palmitoyl groups.<sup>[7]</sup> Although a statistical distribution of the two different groups is obtained, as determined by matrix-assisted laser desorption/ionization time-of-flight (MALDI-TOF) analyses, which implicates a random positioning of these groups, the dendritic scaffold remains monodisperse.

Dendrimer **1** is molecularly dissolved in organic solvents such as tetrahydrofuran (THF) or chloroform, and displays reversible *cis*–*trans* isomerization upon excitation with light with a wavelength of 365 nm. Injection of concentrated solutions of **1** in THF into water (pH 1–8) at 333 K results directly in the formation of opalescent solutions containing vesicles. These vesicles were subsequently investigated by transmission microscopy (TM), scanning fluorescence microscopy (SFM), confocal scanning fluorescence microscopy (CSFM),<sup>[8]</sup> atomic force microscopy (AFM),<sup>[9]</sup> scanning electron microscopy (SEM), and cryo-transmission electron microscopy (Cryo-TEM).<sup>[10]</sup> Transmission microscopy reveals

[\*] Prof. F. C. De Schryver, G. C. Dol, K. Tsuda, M. J. Bartels, T. Asavei, T. Gensch, J. Hofkens, L. Latterini  
 The Department of Chemistry  
 Katholieke Universiteit Leuven  
 Celestijnenlaan 200F, 3001 Heverlee (Belgium)  
 Fax: (+32) 16-32-79-89  
 E-mail: Frans.deschryver@chem.kuleuven.ac.be  
 J.-W. Weener, A. P. H. J. Schenning, Prof. B. W. Meijer  
 Laboratory of Macromolecular and Organic Chemistry  
 Eindhoven University of Technology  
 P.O. Box 513, 5600 MB Eindhoven (The Netherlands)

[\*\*] K.T. thanks the Mitsubishi Paper Mills Co. T.G., J.H., and L.L. thank the European Commission for a TMR fellowship within the frame of the Marie Curie program, the FWO, and the Flemish Ministry of Education, respectively. J.W.W. and A.S. acknowledge grants from the EU (BICEPS project) and the Royal Dutch Foundation of Science, respectively. This work was further supported by DWTC (Belgium), and ESF through SMARTON. An unrestricted research grant from DSM Research is highly appreciated.

the existence of micrometer-sized spherical objects (Figure 1a) that are also visible as bright circular features by SFM using blue light (420–488 nm) for excitation (Figure 1b). The diameters of these objects estimated by both techniques are identical and are all in the 400 nm–20  $\mu\text{m}$  range. Samples containing different size distributions of vesicles could be obtained by microfiltration through regen-

erated cellulose membrane filters with various pore sizes (0.45, 1, 5  $\mu\text{m}$ ).

The AFM and SEM images taken on isolated vesicles obtained from drop-cast, aqueous solutions still show the existence of spheres and oblates in the absence of water (Figure 1c–e), thus confirming the self-stabilizing character of the assemblies. Consecutive AFM scans on the same giant vesicle yielded identical images without significant alteration of the topographic properties. Additional evidence for the stability of these vesicles was obtained by monitoring the change in the turbidity of the vesicle dispersion at  $\lambda = 625\text{ nm}$  on the addition of ethanol. An enhanced stability, relative to that of polymerized vesicle dispersions, was concluded from the observation that the vesicles were stable up to at least 30 vol % of added ethanol.<sup>[11]</sup>

Cryo-TEM and small-angle X-ray scattering revealed the existence of vesicles with a multilaminar, onionlike architecture, from which a bilayer thickness of 5 nm could be estimated (Figure 1f). An interdigitated bilayer structure is proposed (Figure 1g) in which the polar dendrimer part faces the aqueous phase in a highly flattened conformation.<sup>[7]</sup> Computational modeling yielded a length of 32 Å for an alkyl chain containing a *trans*-azobenzene unit and 22 Å for a fully extended palmitoyl chain, and, hence, confirms this arrangement. Additional information on the interdigitated layer structure and stacking of the azobenzene moieties was obtained from the absorption and emission spectra of the vesicles.<sup>[12–14]</sup> A fraction of the azobenzene units within the giant vesicles could be isomerized from the *trans* to the *cis* conformation (360 nm, 2 mW cm<sup>−2</sup>), which indicates that the bilayer structure has sufficient free volume.

CSFM measurements taken on giant vesicles in water confirmed their globular nature and showed there was fluorescence in all the nodal planes through the objects. This latter observation indicates the vesicles are solid spheres, since a series of CSFM images along the axis of the irradiating light gives direct access to the three-dimensional shape of the object as well as the distribution of the fluorescence intensity.<sup>[15, 16]</sup>

Micromanipulation of the vesicles formed by compound **1** is readily achieved by optical trapping.<sup>[17]</sup> In this technique, an object is forced to stay near to the focal point of a highly focused, nonabsorbed beam of light.<sup>[18–21]</sup> Figure 2a displays the TM image which shows a trapped vesicle (encircled), and two vesicles that are immobilized by simple deposition on the surface of the cover glass. In the next images the microscopy stage is moved to the left, and consequently one of the immobilized vesicles hits the trapped vesicle (Figure 2b). The momentum of the immobilized vesicle is large enough to force the trapped vesicle from its original position in a billiardlike fashion. The force acting is in the range of several piconewtons.<sup>[22–24]</sup> Figure 2c clearly shows the displacement of the formerly trapped vesicle, its position is now on the far left of the image. The vesicles still behaved like hard spheres when the microscopy stage was moved at a lower velocity. In these experiments (results not shown) the immobilized vesicle slightly lifted the trapped vesicle. This effect could be observed in the TM image as a change in the contrast of the trapped vesicle. Additional translation of the microscopy

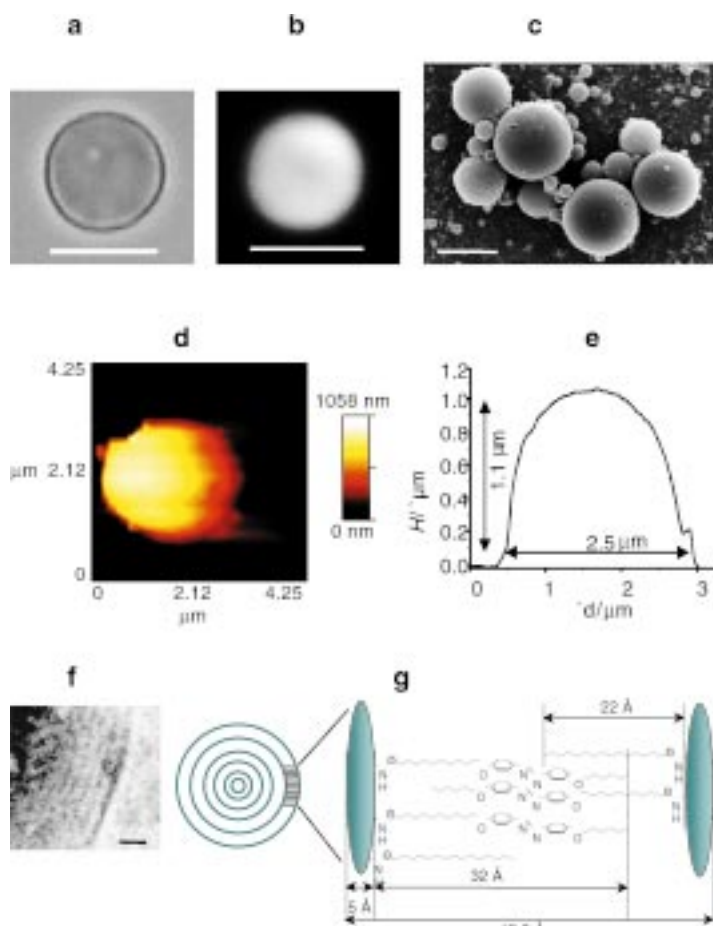


Figure 1. a) Representative TM image of a giant vesicle, which illustrates the spherical structure of the aggregate. A  $100\times$ , 1.3 N.A. oil immersion lens was used in the microscope for imaging. The size of the scale bar is 5  $\mu\text{m}$ . b) CSFM image of the vesicle depicted in (a). The fluorescence originates from stacked azobenzene moieties in the bilayer structure (see (g) for a schematic representation). The size of the vesicle obtained from CSFM (5  $\mu\text{m}$ ) is identical to that of the TM image in (a). The power of the light (420 nm) was  $P_{420} = 25\text{ kW cm}^{-2}$ . c) SEM image of a solvent-cast vesicle solution, which shows vesicles of several sizes. The size of the scale bar is 5  $\mu\text{m}$ . d) Noncontact-mode AFM image of a single vesicle deposited on glass. The image was recorded in the noncontact detection mode using an AFM microscope (Lumina, Topometrix Inc.) with amplitude detection (a commercially available high resonance frequency cantilever was used). The shadow observed on the right of the AFM image is an imaging artifact along the scanning direction (left-to-right). The AFM tip cannot follow the profile at the back edge of the structure because of the sharp topography of the object. e) AFM height profile of the vesicle. The height profile shows that the vesicles residing on the glass surface deform. The width is now roughly twice the height (2 and 1  $\mu\text{m}$ , respectively). f) Cryo-TEM image of a vesicle revealing a clear layered structure. The layer spacing is approximately 5 nm (see also (g)). The size of the scale bar is 12 nm. g) Schematic representation of the interdigitated bilayer based on small-angle X-ray and Cryo-TEM measurements. Additional data from fluorescence measurements proved the presence of stacked azobenzene moieties.<sup>[6]</sup>

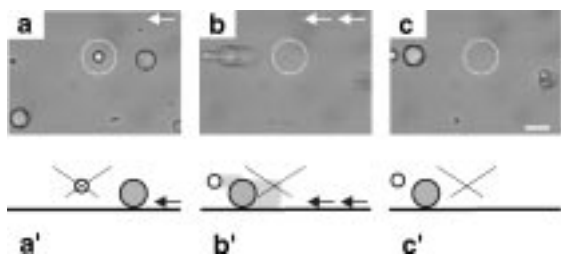


Figure 2. a) TM image of a trapped vesicle (encircled) and two immobilized vesicles. Movement of the sample stage to the left, results in a concurrent motion of the immobilized vesicles. b) On translation of the stage at a high velocity, the trapped vesicle is forced from the trap in a billiardlike fashion. c) This TM image clearly shows the displacement of the previously trapped vesicle. In all images, the dashed circle indicates the position of the trapping beam. a')–c') are schematic representations of the events in (a)–(c). The size of the scale bar is 10  $\mu\text{m}$ . A  $100\times$ , 1.3 N.A. oil immersion lens was used with  $P_{1064}=25\text{ MW cm}^{-2}$  from a Nd-YAG laser.

stage resulted in a shift of the immobilized vesicle concurrent with the movement of the stage, whereas the trapped vesicle regained its original position. The behavior displayed in both these experiments is remarkably different from that of giant unilaminar vesicles investigated thus far which merge upon close contact,<sup>[25]</sup> whereas the vesicles of compound **1** act like hard spheres. The hard-sphere behavior of the vesicles is proposed to result from the unique character of the dendritic building blocks, which can be viewed as oligomeric, head-group-polymerized entities (Figure 1g).

Partial merging of the vesicles can be achieved by local irradiation at the interface of two “touching” vesicles with light with a wavelength of 420 nm (Figure 3). Figure 3a displays two separated vesicles from which the one in the center is optically trapped and therefore bright, while the deposited vesicles, being out of the confocal plane, are seen as opaque. In Figure 3b, the immobilized vesicle is forced against the trapped vesicle. After irradiation with light with a wavelength of 420 nm, both vesicles move concurrently with the cover glass (Figure 3c). Separation of the two vesicles by trapping the top vesicle and movement of the sample stage proved impossible, even when a trapping power of  $250\text{ MW cm}^{-2}$  was used. The CSFM images of the product displayed fluorescence in every nodal plane, including the interface of the two vesicles (Figure 3d). Presumably, irradiation with light with a wavelength of 420 nm leads to local disruptions of the bilayer through isomerization of azobenzene,<sup>[12]</sup> which induces fusion of the outer bilayers of the two vesicles (Figure 3e).

A similar approach was applied to merge small vesicles ( $<500\text{ nm}$ ), which were obtained after filtering the parent dispersion through a filter with a pore size of  $1\text{ }\mu\text{m}$ . In this case, the highly focussed infrared beam forces the vesicles to accumulate near the focus of the beam which results in a very high, local concentration of vesicles in the optical trap.<sup>[26–28]</sup> In accordance with the hard-sphere behavior of the vesicles, the formation of larger

structures did not occur, as evident by transmission microscopy. However, rod-shaped architectures could be obtained upon simultaneous irradiation with light having a wavelength of 420 nm (Figure 4a–4d). The largest rods found were  $11\text{ }\mu\text{m}$  in length with a diameter of  $1\text{ }\mu\text{m}$ , which suggests that at least 10 vesicles were involved in the construction process. The size of the rods depends strongly on the irradiation time used (Figure 4e). The mechanical strength of the rods was tested by pulling the trapped end of a rod, which had been fixed with one end at the surface, until the rod was fully stretched. On further extension, the rod did not rupture, it just sprang from the trap. The rods could be fused to obtain larger rods using a similar strategy. This building process could be repeated several times to yield structures up to  $20\text{ }\mu\text{m}$  in length.

We have shown that irradiation with focussed laser light having a wavelength of 420 nm introduces morphological changes in vesicles of compound **1** as a result of photoisomerization of the azobenzene moieties.<sup>[12]</sup> These changes at the interface of two vesicles presumably lead to interdigitation of the outer layers, and in this fashion a superstructure consisting of several vesicles can be formed. In order to verify this hypothesis we performed similar micromanipulation experiments with two reference compounds: 1) dendrimers functionalized with palmitoyl chains only and 2) dendrimers functionalized entirely with azobenzene-containing alkyl chains. Merging was not observed in manipulation experi-

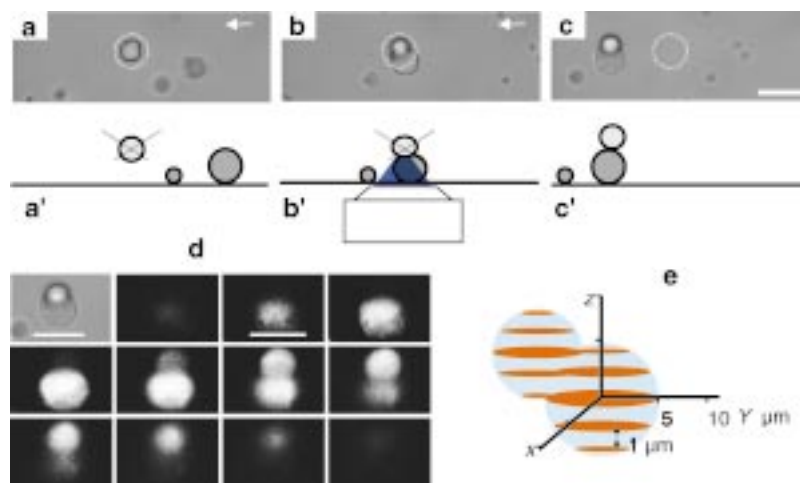


Figure 3. a) TM image of a trapped vesicle (central) floating above the surface of the cover glass, the others are immobilized on the surface. b) Movement of the sample stage to the left results in translation of the immobilized vesicles concurrent with the stage, whereas the trapped vesicle holds its position. The vesicles were kept in this position, and subsequently, the blue light was focussed at the interface of the contact pair. After irradiation for 10 min both lasers were blocked. c) The sample stage was moved to the right, which induced movement of both the immobilized vesicle and the previously trapped one, which proved that the vesicles had merged. The size of the scale bar is  $10\text{ }\mu\text{m}$ . a')–c') are schematic representations of the merging experiment. d) TM image (top left) and CSFM  $z$  slices, recorded after the merging experiment depicted in a)–c). The presence of fluorescence through the complete scan illustrates the existence of ordered azobenzene units within the multilaminar giant vesicle. The fluorescence at the interface of the merged vesicles is evidence for effective interdigitation of the outer layers of the vesicles. The size of the scale bars is  $10\text{ }\mu\text{m}$ , the thickness of each  $z$  slice is  $1.5\text{ }\mu\text{m}$  and  $P_{420}=25\text{ kW cm}^{-2}$ . The apparent height is approximately  $20\text{--}23\text{ }\mu\text{m}$ . By using a calibration factor of  $0.667\text{ }\mu\text{m}$  per  $z$  slice, a diameter of  $13\text{--}15\text{ }\mu\text{m}$  is obtained, which is in good agreement with the estimated value from the individual vesicle dimensions. e) Cartoon of the CSFM experiment in (d), the red disks represent the confocal  $z$  slices.

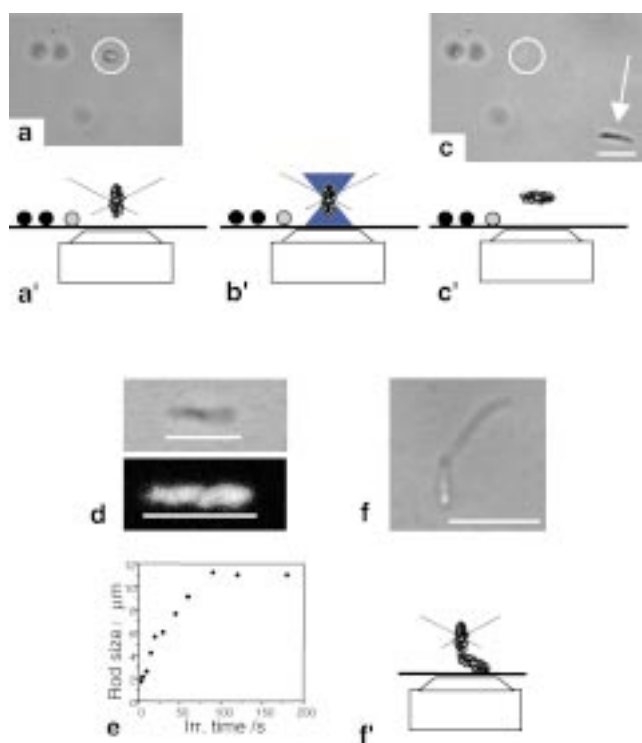


Figure 4. a), c) TM images, and schematic representations (a')–(c') of a merging experiment with small vesicles. In (a), many small vesicles are trapped, and the 420 nm wavelength laser is used subsequently to irradiate the vesicles (schematically represented in (b')). After irradiation both lasers were blocked, and the newly formed rod moves through the solution. The size of the rod is subsequently determined from the image in (c). The arrow points to the formed rod and the open circle indicates the position of the laser beams. In the cartoons (a')–(c'), the crossed, dashed lines indicate the focus of the trapping beam. d) Top: TM image, bottom: SFM image of a merging product. The size of the scale bars is 3.5 μm. Merging:  $t_{\text{irr},420} = 30$  s. e) Plot of the irradiation time ( $t_{\text{irr}}$ ) with light having a wavelength of 420 nm versus the size of the formed rods. The largest rod size found was approximately 11 μm. f) TM image and cartoon of a second merging experiment. The rod was attached onto the surface by descending the focus of the trapping beam until the lower part of the rod was in contact with the surface, thus inducing a fixation after a few seconds. Subsequent irradiation with light (420 nm) triggered a second rod to merge with the head of the immobilized one. The size of the scale bar is 5 μm,  $t_{\text{irr},420} = 60$  s (twice). The same conditions were used in all experiments ( $P_{420} = 25 \text{ kW cm}^{-2}$  and  $P_{1064} = 25 \text{ MW cm}^{-2}$ ).

ments carried out with vesicles prepared from either of these reference dendrimers. In the first case this is the consequence of the absence of photoactive groups, whereas in the vesicles prepared from the second dendrimer the increased order reduces the free volume, and hence photoswitching is hampered. Although a precise molecular picture of the merging of **1** is still lacking, the following experiments show strong evidence for the necessity of a photoinduced process together with a local heating arising from the absorption of the infrared light by the overtone of water to obtain enough flexibility (the system is significantly below its glass-melting temperature  $T_g$ ) for merging. Trapping the vesicles with IR laser light alone without irradiation at 450 nm does not lead to merging. In addition, performing the experiments in  $\text{D}_2\text{O}$ , where the local heating by IR absorption is absent as a result of a frequency shift of the overtone, also does not lead to merging on simultaneous irradiation with IR and UV light.

These results show that by careful design of the dendritic molecule the physical properties of the self-assembled structure can be tuned in such a way that phototriggered micro-manipulation and merging of hard spheres is possible. This possibility leads to the bottom-up synthesis of micrometer-sized objects through a combination of covalent synthesis and supramolecular organization followed by micromanipulation.

Received: December 5, 2000

Revised: February 7, 2001 [Z 16229]

- [1] a) G. R. Newkome, C. N. Moorefield, G. R. Baker, A. L. Johnson, R. K. Behera, *Angew. Chem.* **1991**, *103*, 1205; *Angew. Chem. Int. Ed. Engl.* **1991**, *30*, 1176; b) G. R. Newkome, C. N. Moorefield, G. R. Baker, M. J. Saunders, S. H. Grossman, *Angew. Chem.* **1991**, *103*, 1207; *Angew. Chem. Int. Ed. Engl.* **1991**, *30*, 1178; c) J. K. Young, G. R. Baker, G. R. Newkome, K. F. Morris, C. S. Johnson, *Macromolecules* **1994**, *27*, 3464; d) G. R. Newkome, C. N. Moorefield, *Macromol. Symp.* **1994**, *77*, 63; e) G. R. Newkome, R. Güther, F. Gardullo, *Macromol. Symp.* **1995**, *98*, 467; f) C. J. Hawker, K. L. Wooley, J. M. J. Fréchet, *J. Chem. Soc. Perkin Trans. 1* **1993**, 1287; g) M. E. Piotti, F. Rivera, R. Bond, C. J. Hawker, J. M. J. Fréchet, *J. Am. Chem. Soc.* **1999**, *121*, 9471; h) G. R. Newkome, Z. Yao, G. R. Baker, V. K. Gupta, P. S. Russo, M. J. Saunders, *J. Am. Chem. Soc.* **1986**, *108*, 849; i) A. Schmitzer, E. Perez, I. Ricolattes, A. Lattes, S. Rosca, *Langmuir* **1999**, *15*, 4397; j) A. P. H. Schenning, C. Elissen-Román, J. W. Wecuer, M. W. P. L. Baars, S. van der Gaast, E. W. Meijer, *J. Am. Chem. Soc.* **1998**, *120*, 8199.
- [2] a) J. H. Fuhrop, J. Mathieu, *Angew. Chem.* **1984**, *96*, 124; *Angew. Chem. Int. Ed. Engl.* **1984**, *23*, 100; b) G. H. Escamilla, G. R. Newkome, *Angew. Chem.* **1994**, *106*, 2013; *Angew. Chem. Int. Ed. Engl.* **1994**, *33*, 1937; c) G. R. Newkome, G. R. Baker, M. J. Saunders, P. S. Russo, V. K. Gupta, Z.-q. Yao, J. E. Miller, K. Bouillon, *J. Chem. Soc. Chem. Commun.* **1986**, 752; d) G. R. Newkome, G. R. Baker, S. Arai, M. J. Saunders, P. S. Russo, K. J. Theriot, C. N. Moorefield, L. E. Rogers, J. E. Miller, T. R. Lieux, M. E. Murray, B. Philips, *J. Am. Chem. Soc.* **1990**, *112*, 8458; e) G. R. Newkome, C. N. Moorefield, G. R. Baker, R. K. Behera, G. H. Escamilla, M. J. Saunders, *Angew. Chem.* **1992**, *104*, 901; *Angew. Chem. Int. Ed. Engl.* **1992**, *31*, 917; f) G. R. Newkome, X. F. Lin, C. Yaxiong, G. H. Escamilla, *J. Org. Chem.* **1993**, *58*, 3123; g) G. R. Newkome, X. F. Lin, Y. X. Chen, G. H. Escamilla, *J. Org. Chem.* **1993**, *58*, 7626; h) M. Jørgensen, K. Bechgaard, T. Bjørnholm, P. Sommer-Larsen, L. G. Hansen, K. Schaumburg, *J. Org. Chem.* **1994**, *59*, 5877.
- [3] a) D. A. Tomalia, P. M. Kirchhoff, US-A 4694064, **1987** [*Chem. Abstr.* **1988**, *108*, 56832p]; for excellent reviews on dendronized polymers, see b) A. D. Schlüter, J. P. Rabe, *Angew. Chem.* **2000**, *112*, 860; *Angew. Chem. Int. Ed.* **2000**, *39*, 864; c) A. D. Schlüter, *Top. Curr. Chem.* **1998**, *197*, 165; d) H. Frey, *Angew. Chem.* **1998**, *110*, 2313; *Angew. Chem. Int. Ed.* **1998**, *37*, 2193; e) Z. Bo, J. P. Rabe, A. D. Schlüter, *Angew. Chem.* **1999**, *111*, 2540; *Angew. Chem. Int. Ed.* **1999**, *38*, 2370.
- [4] a) T. M. Chapman, G. L. Hillyer, E. J. Mahan, K. A. Shaffer, *J. Am. Chem. Soc.* **1994**, *116*, 11195; b) I. Gitsov, K. L. Wooley, C. J. Hawker, P. T. Ivanova, J. M. J. Fréchet, *Macromolecules* **1993**, *26*, 5621; c) D. Yu, N. Vladimirov, J. M. J. Fréchet, *Macromolecules* **1999**, *32*, 5186; d) I. Gitsov, J. M. J. Fréchet, *Macromolecules* **1993**, *26*, 6536; e) J. M. J. Fréchet, I. Gitsov, T. Monteil, S. Rochat, J. F. Sassi, C. Vergelati, D. Yu, *Chem. Mater.* **1999**, *11*, 1267; f) J. Iyer, K. Fleming, P. T. Hammond, *Macromolecules* **1998**, *31*, 8757; g) J. Iyer, P. T. Hammond, *Langmuir* **1999**, *15*, 1299; h) J. C. M. Van Hest, D. A. P. Delnoye, M. Baars, M. H. P. Van Genderen, E. W. Meijer, *Science* **1995**, *268*, 1592; i) J. C. M. Van Hest, D. A. P. Delnoye, M. W. P. L. Baars, C. Elissen-Román, M. H. P. van Genderen, E. W. Meijer, *Chem. Eur. J.* **1996**, *2*, 1616; j) J. N. Israelachvili, D. J. Mitchell, B. W. Ninham, *J. Chem. Soc. Faraday Trans. 2* **1976**, *72*, 1525; k) J. C. M. Van Hest, M. W. P. L. Baars, C. Elissen-Román, M. H. P. Van Genderen, E. W. Meijer, *Macromolecules* **1995**, *28*, 6689.
- [5] a) I. Gitsov, K. L. Wooley, J. M. J. Fréchet, *Angew. Chem.* **1992**, *104*, 1282; *Angew. Chem. Int. Ed. Engl.* **1992**, *31*, 1200; b) I. Gitsov, J. M. J. Fréchet, *J. Am. Chem. Soc.* **1996**, *118*, 3785.



- [6] a) K. Ichimura, S.-K. Oh, M. Nakagawa, *Science* **2000**, 288, 1624; b) J. W. Weener, E. W. Meijer, *Adv. Mater.* **2000**, 12, 741.
- [7] A. P. H. J. Schenning, C. Elissen-Román, J. W. Weener, M. W. P. L. Baars, S. J. van der Gaast, E. W. Meijer, *J. Am. Chem. Soc.* **1998**, 120, 8199.
- [8] T. Gensch, J. Hofkens, J. van Stam, H. Feas, S. Creutz, K. Tsuda, R. Jerome, H. Masuhara, F. C. De Schryver, *J. Phys. Chem. B* **1998**, 102, 8440.
- [9] *Procedures in Scanning Probe Microscopies*, Wiley, Chichester, **2000**.
- [10] B. M. Discher, Y.-Y. Won, D. S. Ege, J. C.-M. Lee, F. S. Bates, D. E. Discher, D. A. Hammer, *Science* **1999**, 284, 1143.
- [11] H. Hub, B. Hupfer, H. Koch, H. Ringsdorf, *Angew. Chem.* **1980**, 92, 962; *Angew. Chem. Int. Ed. Engl.* **1980**, 19, 938.
- [12] K. Tsuda, G. Dol, T. Gensch, J. Hofkens, L. Latterini, J. W. Weener, E. W. Meijer, F. C. De Schryver, *J. Am. Chem. Soc.* **2000**, 122, 3445.
- [13] M. Shimomura, R. Ando, T. Kunitake, *Ber. Bunsenges. Phys. Chem.* **1983**, 87, 1134.
- [14] M. Shimomura, T. Kunitake, *J. Am. Chem. Soc.* **1987**, 109, 5175.
- [15] S. R. McAlpine, S. L. Schreiber, *Chem. Eur. J.* **1999**, 5, 3528.
- [16] F. M. Menger, A. Archut, *Acc. Chem. Res.* **1998**, 31, 789.
- [17] F. M. Menger, J. S. Keiper, *Adv. Mater.* **1998**, 10, 888.
- [18] A. Ashkin, *Phys. Rev. Lett.* **1970**, 24, 156.
- [19] A. Ashkin, J. M. Dziedzic, J. E. Bjorkholm, S. Chu, *Opt. Lett.* **1986**, 11, 288.
- [20] K. Svoboda, S. M. Block, *Annu. Rev. Biophys. Biomol. Struct.* **1994**, 23, 247.
- [21] L. I. McCann, M. Dykman, B. Golding, *Nature* **1999**, 785.
- [22] C. D'Helon, E. W. Dearden, H. Rubinshtein-Dunlop, N. R. Heckenberg, *J. Mod. Opt.* **1994**, 41, 595.
- [23] M. E. J. Friese, H. Rubinshtein-Dunlop, N. R. Heckenberg, E. W. Dearden, *Appl. Opt.* **1996**, 35, 7112.
- [24] R. M. Simmons, J. T. Finer, S. Chu, J. A. Spudich, *Biophys. J.* **1996**, 70, 1813.
- [25] J. D. Moroz, P. Nelson, R. Bar-Ziv, E. Moses, *Phys. Rev. Lett.* **1997**, 78, 386.
- [26] P. Borowicz, J. Hotta, K. Sasaki, H. Masuhara, *J. Phys. Chem. B* **1998**, 102, 1896.
- [27] J. Hofkens, J. Hotta, K. Sasaki, H. Masuhara, T. Taniguchi, T. Miyashita, *J. Am. Chem. Soc.* **1997**, 119, 2741.
- [28] J. Hofkens, J. Hotta, K. Sasaki, H. Masuhara, K. Iwai, *Langmuir* **1997**, 13, 414.

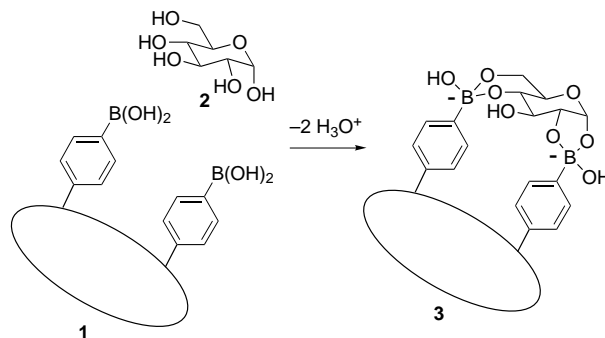
## Computer-Guided Design in Molecular Recognition: Design and Synthesis of a Glucopyranose Receptor\*\*

Wei Yang, Huan He, and Dale G. Drueckhammer\*

The design of compounds which are capable of specific recognition of molecules and ions is a long-standing challenge in organic chemistry. In addition to its fundamental interest, this work is of increasing practical value in the development of chemosensors for compounds of biological and environmental importance<sup>[1]</sup> and is a key element of biomimetic catalysis.<sup>[2]</sup> The specific binding of one compound from a complex

mixture generally requires the interaction of multiple functional groups of the receptor with complementary functionality of the guest compound.<sup>[3, 4]</sup> Good affinity and selectivity requires the precise placement of the recognition elements of the receptor in the proper position and orientation for optimal complementarity to the guest. Nature uses proteins (enzymes, antibodies, and other protein-based receptors) as a basis for specific receptors. Efforts to achieve specificity and affinity in smaller synthetic molecules has relied primarily on intuition for the identification of molecular scaffolds that would permit proper orientation of the functionality for molecular recognition. We envisioned that the computer program CAVEAT, developed by Bartlett and co-workers and previously utilized for the design of enzyme inhibitors and conformationally constrained peptides, could serve as a valuable tool for the discovery of molecular backbones for the orientation of functional groups for molecular recognition.<sup>[5, 6]</sup> Described here is the demonstration of a CAVEAT-based design approach in the development of a glucopyranose receptor incorporating precisely positioned arylboronic acid groups as recognition elements.

Arylboronic acids have long been known to form stable complexes with sugars and other diols in aqueous solution.<sup>[7]</sup> Numerous arylboronic acids have been prepared and studied as sugar receptors, and those incorporating fluorescent aryl groups have been explored as fluorescence-based sugar sensors.<sup>[8–15]</sup> Of particular interest are glucose sensors for potential application in the maintenance of blood glucose levels in persons with diabetes.<sup>[16, 17]</sup> However, the simple arylboronic acids form stable complexes with a variety of sugars and thus are not useful as specific receptors or sensors for a single sugar. Compounds have been prepared that contain a pair of arylboronic acid groups in somewhat flexible structures which form two cyclic boronates with a single sugar molecule.<sup>[11–14]</sup> These bis-boronic acids, while not designed for complexation with a specific sugar, have demonstrated somewhat enhanced, though still modest, selectivity. A glucopyranose receptor **1** containing a pair of precisely positioned phenylboronic acid groups was chosen as an initial target for receptor design using CAVEAT (Scheme 1). The large oval structure in **1** represents a polycyclic organic framework to be identified using CAVEAT. Since glucopyranose **2** can form cyclic boronates between the  $\alpha$ -1,2 and 4,6-hydroxy groups,<sup>[14, 18]</sup> the receptor was designed to incorporate arylboronic acid groups in the proper relative position to form a



Scheme 1. Complex formation between glucose and a bis-arylboronic acid.

[\*] Prof. D. G. Drueckhammer, W. Yang, H. He  
Department of Chemistry  
State University at Stony Brook  
Stony Brook, NY 11794-3400 (USA)  
Fax: (+1) 631-632-7960  
E-mail: dale.drueckhammer@sunysb.edu

[\*\*] This work was supported by the National Institutes of Health (grant DK5523402).